Interrelation of Structure and Operational States in Cascading Failure of Overloading Lines in Power Grids

Fei Xue, Ettore Bompard, Tao Huang, Lin Jiang, Shaofeng Lu, Huaiying Zhu

Abstract—As the modern power system is expected to develop to a more intelligent and efficient version, i.e. the smart grid, or to be the central backbone of energy internet for free energy interactions, security concerns related to cascading failures have been raised with consideration of catastrophic results. The researches of topological analysis based on complex networks have made great contributions in revealing structural vulnerabilities of power grids including cascading failure analysis. However, existing literature with inappropriate assumptions in modeling still cannot distinguish the effects between the structure and operational state to give meaningful guidance for system operation. This paper is to reveal the interrelation between network structure and operational states in cascading failure and give quantitative evaluation by integrating both perspectives. For structure analysis, cascading paths will be identified by extended betweenness and quantitatively described by cascading drop and cascading gradient. Furthermore, the operational state for cascading paths will be described by loading level. Then, the risk of cascading failure along a specific cascading path can be quantitatively evaluated considering these two factors. The maximum cascading gradient of all possible cascading paths can be used as an overall metric to evaluate the entire power grid for its features related to cascading failure. The proposed method is tested and verified on IEEE30-bus system and IEEE118-bus system, simulation evidences presented in this paper suggests that the proposed model can identify the structural causes for cascading failure and is promising to give meaningful guidance for the protection of system operation in the future.

Index Terms—Cascading Failure, Complex Network, Cascading Path, Cascading Drop, Cascading Gradient

1. Introduction

As one of the most important public facilities, power system plays a critical role for modern society and economy. With great development in information and control technologies, it is expected to be upgraded to a new generation, i.e. smart grid or energy internet. However, on the other hand, failures in power system may cause more and more catastrophic consequences as observed from several historical outages in US and Europe [1]. Based on the analysis of historical records, cascading failures can make more serious impacts on social economy and living [2].

Cascading outage or failure is a sequence of events in which an initial disturbance, or a set of disturbances, triggers a sequence of one or more dependent component outages [2].The propagation process of cascading failure is very complex by involving power transmission and distribution, protection system, control system, information system and even human decision-making process. Therefore, although people have made great progress in revealing mechanism of cascading failure and mitigate its risks [2]-[13], there are still no ultimate solutions. Although some of these methods have considered the problem based on both real operational states and structural factors for evaluation, the impact of states and structures have not been clearly distinguished and quantitatively evaluated respectively. Furthermore, it is still difficult for them to overcome the heavy computation burden and stochastic causal relations.

After the investigation of small-world [14] and characterization of scale-free networks [15] in power grids, complex networks(CN) have been widely studied for the analysis about power grid security [16]-[20].Meanwhile, CN is also popularly applied in studying cascading failures of network systems including power grids. For isolated networks, the study of cascading failure in CN mainly falls into two categories [21]: first, failures due to network overload when the network flow is a physical quantity; second, models based on local dependences, such as the decision-making process of interacting agents. Furthermore, as many network systems are tightly related, a research framework for robustness of interdependent networks was also proposed [21]. As discussed above, the real cascading process of power grids is very complicated by involving different interdependent systems.

Fei Xue and Shaofeng Lu are with the Department of Electrical and Electronic Engineering, Xi'an Jiaotong-Liverpool University, No. 111 Ren'ai Road, Suzhou Industrial Park, Suzhou, P.R. China (phone: +86 512 8816 1409; e-mail: Fei.Xue@xjtlu.edu.cn).

Ettore Bompard and Tao Huang are with Politecnico di Torino in Italy.

Lin Jiang is with the University of Liverpool in United Kingdom.

Huaiying Zhu is with the SDIC Baiyin Wind Power Co., LTD. in China

But if the study focuses on the cascading process due to line overloading, that falls into the first category where the networks are isolated. In this category, by considering betweenness as a type of load, a well-known cascading failure model was developed in CN [22]-[24]and applied to study power grids[25][26]. However, these models and methods were based on some assumptions which are not acceptable from the viewpoint of electrical engineering. Therefore, extended topological approaches were developed by taking into account both structural features and physical rules of electrical engineering [27]-[29]. Based on these approaches, the concept of betweenness was updated as an extended version by taking into account Power Transmission and Distribution Factors (PTDF) and transmission capacities [30]. Some works adopted in this updated betweenness with the former cascading model to study power grids[31]-[33], but they still cannot overcome the inconsistency between this cascading failure model and the real physical features in power grids, which will be discussed in later sections in this paper.

Generally speaking, the progress in network science in recent years implies that the structure of power grids can possibly provide some inherent information related to cascading failures and thus mitigate the difficulties in analyzing them. However, up to date, existing models based on CN were not sufficiently unified and not convincing enough due to some unacceptable assumptions in the model, such as loads, line capacity and tolerance factor, and confusion between the structure features and operational states. Most of them can only provide some statistical results which can be inapplicable and hard to be verified for practical system operations.

This paper proposes a framework for the analysis of cascading failures by distinguishing the effects of structural features and operational states and provides quantitative indicators for system operations to prevent and defend cascading failures. For structure analysis, cascading paths will be identified by extended betweenness and quantitatively described by cascading drop and cascading gradient. Furthermore, the operational state for cascading paths will be described as the loading level. Then, the risk of cascading failure along a specific cascading path can be quantitatively evaluated by an integration of these two factors. The maximum cascading gradient of all possible cascading paths can be used as an overall metric to evaluate the whole power grid for its feature about cascading failure. The proposed methodology is tested on IEEE30-bus system and IEEE118-bus system, the simulation results indicates that the method is effective to identify the structural causes for cascading failure and can provide meaningful guidance for the protection of system operation.

2. DISCUSSION ON FORMER CASCADING FAILURE MODELS

In complex networks, a networked system of power grid can be modeled as a graph $Y=\{B,L\}$. B ($\dim\{B\}=N_B$) is the set of vertices (or nodes), L ($\dim\{L\}=N_L$) is the set of edges (or lines). In the well-known former work about cascading failures in CN[23][25], the load of an edge was considered as the betweenness of that. By its initial definition in CN, betweenness is the total number of shortest paths passing through the edge l:

$$B_l = \sum_i^{N_B} \sum_j^{N_B} \frac{\sigma_{ij}(l)}{\sigma_{ij}} \ \ l \in L \ \ i \neq j \in B \qquad (1)$$

where σ_{ij} is the total number of shortest paths connecting vertices i and j, $\sigma_{ij}(l)$ denotes the number of shortest paths between i and j that pass through l.

In the proposed model in [23][25], the load of an edge was regarded as its betweenness. The capacity of l is defined as the maximum load (betweenness) that l can handle:

$$C_l = \alpha B_l(0) \qquad (2)$$

where $B_l(0)$ is the load (betweenness) at initial time step 0, and $B_l(t)$ denotes the load at time step t. α is the tolerance parameter which is based on the assumption that the capacity should be proportional to the initial load. To simulate a process of cascading failure using this model, an edge could be supposed to be cut off due to stochastic failure or intentional attack. After that, the change of load (betweenness) following structure variation will be recalculated and compared with the limits defined in (2). For any line detected with load (betweenness) higher than the corresponding limit, this line will be flagged as failed and removed from further calculations. This process will continue until the stopping criterion is met to model a cascading failure process.

This model has been applied to study cascading failures for power grids [25][26], where some nodes or edges are attacked or removed at time step t, the betweenness distribution was recalculated as $B_l(t+1)$ for the next step. If the updated load $B_l(t+1)$ exceeds capacity limit C_l, line l will be cut off and this procedure will further be proceeded. For power grids, this model has the following defects which may not be acceptable for electrical engineering.

1. In the initial definition of betweenness, transmission of physical quantity is only considered through the shortest path. This is inconsistent with the fact that most paths in power grids are involved in power transmission between two buses.

2. Load is defined as betweenness in the proposed model. In fact, betweenness is a characteristic completely determined by structure. In power system, the load of transmission line is the exact power flow through it which is a totally different concept from betweenness.

3. Capacity is defined proportional to the initial betweenness. In power grids, capacity of a line is the maximum power through it according to its physical feature and protection settings, which has nothing to do with betweenness and tolerance parameter in (2).

4. The propagation process is based on the failures arising when betweenness exceeds the capacity C_l. However, cascading failure of transmission line in power grid is caused by overloading of the line. Betweenness is a feature depending on structure but not operational states, and power flow is an indicator of operating state of the network. Even in a power grid with no power flow,

betweenness and this modeling procedure can still exist, so it cannot really reflect the mechanism of cascading failures.

To overcome the defects in initial definition of betweenness, an extended version of betweenness for power grids was proposed in [30]. In the linear model of power systems, Power Transfer Distribution Factors (PTDFs) is used to evaluate the contribution of each transmission line in power transmission. PTDFs can indicate the sensitivity of the power through each line for a power injection/withdrawal between a couple of buses. PTDFs can be represented by a $N_L \times N_B$ matrix $\boldsymbol{F}$ whose element f_{lj} represents the change of power on line l for a unit change in power injection at bus j and withdrawal at the reference bus. f_l^{gd} is the change of the power on line l ($l \in L$)for a unit change injection at generation bus g and withdrawal at load bus d:

$$f_l^{gd} = f_{lg} - f_{ld} \ \ l \in L \tag{3}$$

Therefore, PTDF completely depends on structure and impedance of network components and is independent from operational states.

Due to physical features of transmission lines and requirement of stability and security for power system, each line has its maximum transmission limit P_l^{max}, which is different from the capacity defined in (2). This line flow limit will impose constraints on power transmission between any pair of buses; this can be described as the power transmission capacity M_g^d which is the power injection at generation bus g and withdrawn at load bus d when one of the lines connecting g and d *first* reaches its limit P_l^{max}:

$$M_g^d = \min_{l \in L}\left(\frac{P_l^{max}}{|f_l^{gd}|}\right) \tag{4}$$

Based on the discussion above, the line betweenness in power grids can be redefined as:

$$T_l = \max[T_l^P, |T_l^N|] l \in L \tag{5}$$

T_l^P and T_l^N respectively indicate the positive and negative betweenness:

$$T_l^P = \sum_{g \in G} \sum_{d \in D} M_g^d f_l^{gd}, \ if f_l^{gd} > 0 \tag{6}$$

$$T_l^N = \sum_{g \in G} \sum_{d \in D} M_g^d f_l^{gd}, \ if f_l^{gd} < 0 \tag{7}$$

$M_g^d f_l^{gd}$ represents the maximum contribution of line l for power transmission from bus g to bus d.

This definition has overcome the defect 1 by taking into account the contributions of all lines and paths in power transmission and considering the different flow limit of each line. Some works have been done by integrating this extended betweenness with the former cascading failure model [31]-[33]; however, defects 2, 3 and 4 still exist or are not completely solved.

3. STRUCTURAL FEATURES AND OPERATIONAL STATES

Betweenness in its original definition in CN is an indicator for how much a component is responsible for the functionality of the whole network based on the structure of the network. Similarly, the extended betweenness defined in (5) still depends on structure features of power grids and is independent from the operational states, it indicates how much a transmission line is responsible for the overall power transmission function of the network. However, the defects discussed above for former cascading failure models[22][24][30]-[32] mixed this structural metric with operational states in defining load, capacity and propagation process. Impacts from structural features and operational states cannot be clearly distinguished and evaluated.

TABLE I
STRUCTURAL FEATURES AND OPERATIONAL STATES

Structural features	Operational states
Connection of nodes and lines.	Power injection of generation buses.
Distribution of generation buses and load buses.	Power consumption on load buses.
Line flow limits and impedance.	Corresponding power flow through each line.

The different roles of structure and operational states in analysis of power system security were originally proposed in [29]. We can use the following example to explain their relations:
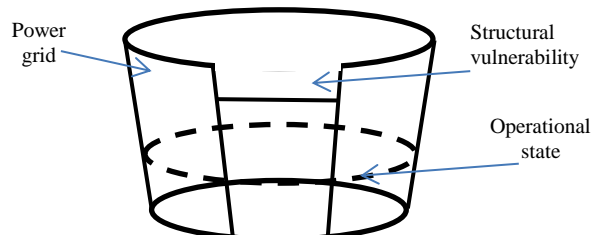
Fig. 1 Structure and operational states

Figure 1 is a schematic figure to illustrate the Cask Effect. In fact, we can imagine the cask as power grid, and its capability for functionality, i.e. its volume, completely depends on its structure even there is no water inside. The level of water can be considered as the operational state of grids, just like the power flow in power grids. The short slab is the vulnerability caused by its structure. However, this vulnerability will have an impact on the functionality of the cask only when the water level is higher than the short slab. Therefore, structure vulnerability is caused by structural features but its risk of impact on network functionality also depends on the operational states. In the field of cascading failures in power grids, people have realized that structural vulnerabilities may be part of its deep reasons, but the works up to date have not successfully distinguished and analyzed them.

The identification of structure and operational features depends on the available details of power system model. If we adopt a linear power system model for DC power flow calculation, the structural features and operational states can be summarized as shown in Table I. Besides the topological connection of all buses and lines, the types and distribution of buses are also structure features. As described in (6) and (7), the locations of generation buses and load buses will influence the calculation of extended betwenness and capacity M_g^d. Furthermore, the impedance and line flow limit of each line are also definite physical features independent from operational states. The calculation of PTDF and capacity M_g^d will be influenced by them. In the meantime, the power injected from each generation bus, and the power withdrawn to each load bus and the corresponding power flow may keep changing during system operations, which together describe the operational state of power grids, just like the water level of the cask.

In former studies, the impacts of structure and operational states in the process of cascading failure were not clearly distinguished and analyzed. The first contribution of this paper is to construct an evaluation framework where the structure and operational state are the two different factors influencing cascading failure and will be analyzed respectively. Furthermore, they are also related and jointly leading to the exact cascading process. Therefore, metrics of these two factors should be integrated based on specific mechanism to jointly indicate the corresponding risk of cascading failure.
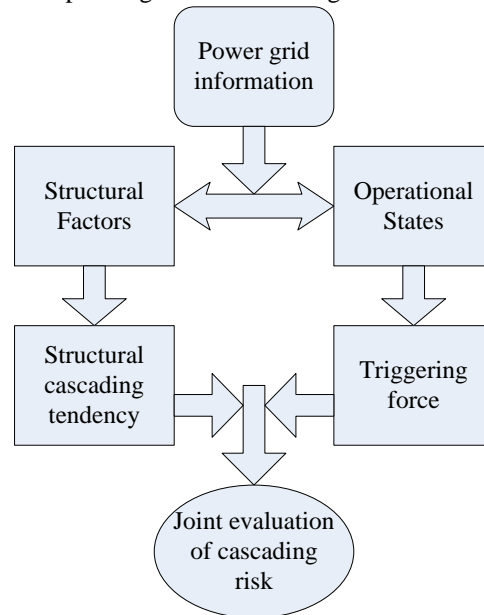

Fig. 2 Framework for cascading failure analysis.

Figure 2 is a diagram for the proposed framework. The mechanism of cascading failure can be considered as analogy with an object falling down along a slope. This process depends on two independent but closely related factors, i.e. the falling down tendency caused by the structure of slope (higher tendency for steeper slope) and a triggering force which may push the object down. Therefore, in cascading failure of power grids, there is also a cascading tendency depending on the original structure of the networks and a triggering force depending on the operational states. With given information about a power gird, the structure factors and operational states can be decomposed like table 1. Furthermore, according to the structure factors, metrics to evaluate the corresponding cascading tendency should be developed, i.e. the "structural" metrics, and metrics for the corresponding triggering force based on operational states, i.e. the "operational" metrics, should also be defined based on which the cascading risk should be jointly assessed.

Under this framework, the second contribution of this paper is to define a cascading path which is quantitatively evaluated by the above-mentioned structural metrics and operational metrics. The product of these two metrics defined as the cascading risk will indicate the exact risk of cascading failure along the corresponding cascading path. The following two sections will introduce these

two metrics respectively and how they jointly define the cascading risk. Together with the results of case study, the paper also intends to make the following three statements.

First, some important features of cascading failures (cascading tendency) may only depend on network structures not operation states;

Second, the exact triggering of cascading failures depends on both structure and operational states, but their effects could be evaluated respectively;

Third, with features captured from structural analysis, it is possible to improve network structure to reduce cascading risk, or to give suggestions to prevent cascading failures.

4. CASCADING PATH

To capture the structure vulnerabilities for cascading failures, we still begin our illustration from betweenness. As discussed in Sec. II, the extended betweenness can indicate how much a transmission line is responsible for the overall functionality of the whole power grid. Therefore, if a line is removed, its responsibility will be taken by the other remaining lines. Correspondingly, after recalculation after the removal of a line, the new betweenness of each line can be obtained (mostly increased but also possibly decreased compared with the initial network structure). Therefore, the cumulative change of betweenness of line l after another line k is removed at time step t ($t=1$ at beginning) can be defined as the drop of l:

$$D_l(t) = [T_l(t) - T_l(0)]/P_l^{max} \qquad (8)$$

This is to indicate the change of betweenness with reference to the initial structure and normalized by its line flow limit. It is important to clarify that sometimes some line loading for a particular line may decrease when some other lines are removed from the grid. So the drop defined in (8) may be non-monotonic, and either positive or negative. Large positive $D_l(t)$ generally means a tight dependency of responsibilities between l and the former removed line set H (for example $H=\{k\}$ at beginning), l can be called as a dependent line of H. Therefore, a large positive value of $D_l(t)$ may indicate that during operation a large part of power flow on H may possibly be taken by l when all lines in H are removed, and so line l has a high risk to be further removed because its power flow is more likely to exceed its line flow limit.

However, betweenness and $D_l(t)$ can only give quantitative evaluation for this tendency, the real failure of a line should be determined by its real power flow compared with line flow limit. After all lines in H are removed, there are possibly multiple lines with large positive $D(t)$ regarded as the dependent lines, and they are considered to be with higher tendency to be further removed. If we select one dependent line from them, for example l, and suppose it is removed due to large $D_l(t)$ on the next time step and H is extended by including line l, other dependent lines for H (for example $H=\{k, l\}$) can be further identified. This process may further continue for several time steps with selected dependent lines removed on each step, and H is extended by including the former removed lines step by step. Therefore, a sequence of dependent lines will be identified with corresponding drop on each step, for example:

$$k \to l \ [D_l(1)] \to m \ [D_m(2)] \to n \ [D_n(3)] \to q[D_q(4)]\ldots\ldots$$
$$H=\{k,l,m,n,q\ldots\ldots\}$$

Such a sequence of dependent lines are defined as a cascading path H, and the total number of time steps is defined as its length N^H, the drop of the last line in the path with reference to its initial extended betweenness is defined as the cascading drop of this path D^H.

As shown in figure 3, the cascading path can be imagined as a path on a slope. The drop of the path can be considered as the drop of the slope from the ground level. Therefore, the cascading tendency of the cascading path can be defined as the cascading gradient of the path:
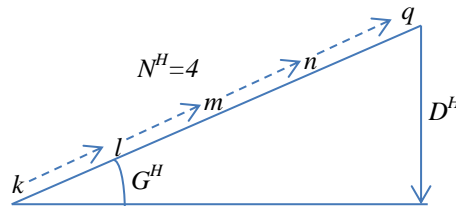
$$G^H = D^H/N^H \qquad (9)$$

Fig. 3 Sketch for cascading path.

If two cascading paths have different length, such as:

$$k \to l \ [D_l(1)] \to m \ [D_m(2)] \to n \ [D_n(3)] \to q[D_q(4)]$$
$$k \to s[D_s(1)] \to r \ [D_r(2)] \to e \ [D_e(3)]$$

It is not meaningful to directly compare their cascading drop, but cascading gradient for different paths with different length can be

compared to indicate their extents of tendency, because longer length will accumulate larger cascading drop.

In searching cascading paths for a power grid, the searching process will be stopped when the network is decomposed into non-connected sub-networks. If the network is partitioned into two non-connected sub-networks, the calculation process can be repeated for each sub-network as a new network structure to obtain the information for further propagation.

For a power grid Y, if **CP is to** denote its all possible cascading paths, the maximum cascading gradient among **CP** is defined as the cascading gradient of the whole network:

$$G^Y = \max_{H \in CP} G^H \tag{10}$$

So G^Y is an indicator for a power grid to describe its structural vulnerability for cascading failure. It is necessary to point out that the cascading drop and cascading gradient calculated for two networks of different scales may not be directly compared. The betweenness calculated by equation (6) and (7) are based on accumulation of all possible generation-load pairs. Networks of different scales may have very different number of generation-load pairs. For network A and network B, if their total number of generation-load pairs are GL_A and GL_B respectively, then the cascading gradient in network B can be converted with reference to network A using (11):

$$G_A^H = G_B^H \times \left(\frac{GL_A}{GL_B}\right) \tag{11}$$

According to the definition of cascading path, in theory, any combination of lines in sequence can be considered as a cascading path. Therefore, for a large-scale power grid, to search and calculate its all possible cascading paths would be a computationally prohibited task. .

In fact, in our analysis, we are only interested in cascading paths with a large cascading drop and gradient. Therefore, during the search process of cascading path, a threshold value T_D for single step drop can be defined. Only lines with single-step drops higher than this threshold value will be considered for further calculation. Single-step drop for line l is defined as:

$$D_l^s(t) = [T_l(t) - T_l(t-1)]/P_l^{max} \tag{12}$$

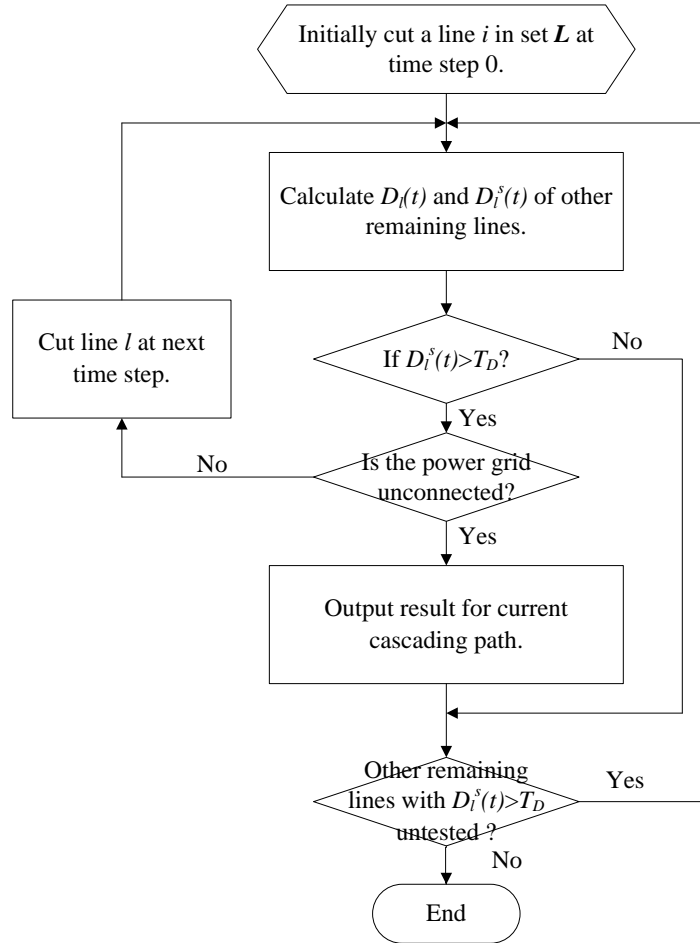The whole searching process can be indicated as figure 4.

Fig. 4 Flowchart for the algorithm of cascading path searching.

Initially, each line of the power grids will be cut off in turn with others connected. After cutting one line at time step 0, the drop of other remaining lines will be calculated by equation (8) and (12). These remaining lines will be tested one by one. If the drop of

one line l at a single step $D_l^s(t)=[T_l(t)-T_l(t-1)]/P_l^{max}$ is higher than the threshold T_D, and the power grid is still connected as one network, this line l will be further cut off on next time step and l will be included in the searching cascading path. This process will continue until the network is discomposed into two disconnected networks and the lines in cutting sequence can be considered as one cascading path. During this process, if the drop of one line l at a single step is lower than the threshold $D_l^s(t)<T_D$, the searching for this cascading path will be stopped and return with no result. This is because a cascading failure propagation is a series events; low drop at single step means low possibility for further propagation. If multiple lines satisfying $D_l^s(t)>T_D$, each will be considered to develop a new cascading path. After finishing calculating one cascading path, all other remaining untested lines at each step with $D_l^s(t)>T_D$ will be further tested by constructing another new cascading path respectively. Only when all remaining lines at all time steps are tested and all their single step drops are lower than T_D, or an islanded sun-network is detected, the searching process will be stopped. With a proper setting of threshold, this algorithm can greatly improve its computational efficiency and find out all possible cascading paths with drops higher than the threshold value.

To avoid impacts of inappropriate T_D, the number of paths N_T in the targeted top ranking paths should firstly be set; then a step decay ΔT is defined. Then a new threshold value $T'_D = T_D - \Delta T$ can be reset and the calculation in figure 4 can be repeated. This process can be stopped when the detected N_T top ranking cascading paths by T'_D and T_D respectively keep unchanged. The corresponding identified top ranking cascading paths then can be considered stable.

It is important to clarify that the algorithm in figure 4 is to detect the structure vulnerability of cascading failure by cascading paths with the cascading gradient, but not to simulate exact process of cascading failure. This is similar to detect the steepest paths of a given mountain according to structure, but not to exactly tell if an object will really fall down along this path. The real process of cascading failure can be simulated by accurate calculation of power flow with given operational states compared with power flow limits of corresponding lines, which will be applied to verify the effectiveness of the detected cascading paths in the following case study.

5. LOADING LEVEL AND CASCADING RISK

As we have discussed above, the cascading gradient and cascading drop for a cascading path can only indicate the tendency of changing in responsibilities of lines due to the change of structure. With high gradient and drop, the corresponding increase in power flow would be possibly higher. However, like figure 1, this is only a structural vulnerability; the occurrence of cascading failure will also depend on the power flow level. In an extreme example, if there is no power flow in the whole power grid, no cascading failure can be triggered no matter how high the gradient and drop are.

Generally speaking, when a cascading path is identified with a high gradient, if the power flow in all the lines of this path is close to their power flow limit, the power flow of the first removed line k will be largely taken by other lines with high drop $D_l(t)$ (such as l in figure 2) due to the structural rules described by cascading drop. Since the original load level of l is also heavy, this has a high possibility to make the power flow of l exceed its flow limit and to be further removed. Therefore, a cascading failure has a high possibility to be triggered along this cascading path.

Therefore, we can define the loading level of a cascading path H under state S as:

$$L_S^H = \frac{1}{n}\sum_{l\in H}\frac{P_l}{P_l^{max}} \qquad (13)$$

where n is the number of lines in H, P_l is the actual power flow in line l.

As we have discussed, the real cascading risk depends on two aspects, i.e. the structural vulnerability and corresponding operational state. Here we propose an evaluation framework, where the structural vulnerability can be indicated by the identified cascading paths with large gradient and the operational state of such paths can be described by their loading level. Hence we can define the cascading risk along an identified cascading path H under state S as:

$$R_S^H = G^H \cdot L_S^H \qquad (14)$$

With the same cascading gradient, higher loading level would be with higher risks of failure; with the same loading level, higher gradient would be more likely to fail. We can consider two extreme situations as follows:

1. If the cascading gradient of a path is zero, meaning when the former line is removed, there will be no change in power transmission responsibilities for other lines. So even the loading level is extremely high (but still lower than P_l^{max}), no cascading failure will be triggered.

2. If the loading level is zero, meaning there is completely no power flow in the network, even the cascading gradient is high, no cascading failure will be triggered.

The real situation may be between these two extreme cases. This assessment framework has the following applications.

1. For a typical network structure, cascading paths with higher cascading gradients can be identified in advance; loading level and cascading risk for these paths can be monitored during system operation. Just like discussion for figure 2, a system operator operating power system can be imagined as a driver driving a car on mountain slope. The steepest paths are determined by the mountain structure, but the driver should control the car to avoid these dangerous paths.

2. Cascading gradient for a network in (10) can be used to assess the vulnerability of a network for cascading failure; different network structures can be directly compared. This can be utilized for power grid planning and design.

3. Measures to improve the structural vulnerabilities or attacking strategies can be quantitatively assessed by comparing network gradient before and after the structure changing.

To compare with the former models in [21]-[26], we assume there are two cascading paths indicated as: l_1->l_2->l_3->l_4, and l_1->l_5->l_6->l_7. If l_1 has been initially cut off, and then the betweenness of l_2 and l_5 both increase significantly. In the models proposed in [21]-[26], these increased betweenness will be compared with the limits defined in (2); and if they both exceed the limits, they will be regarded broken and invalid for further propagation. However, in the model of this paper, the increase of betweenness in both lines will be characterized by the cascading drop which only indicates the failure tendency due to structure. For example, if the loading level of l_2 is quite low and the loading level of l_5 is quite high, a cascading failure will be more likely to propagate through the second path, but not the first one. Similarly, for the second path, if the loading levels of l_5 ,l_6 and l_7 are all quite high, the failures of these three lines may happen simultaneously.

Furthermore, due to uneven distribution of PTDF, the loading levels of lines in the same cascading path may be very different. For example, a cascading path with loading level of each line in percentage is indicated as : l_1(100%)->l_2(30%)->l_3(20%)->l_4(10%), the average loading level for the whole path is only 40%. But since the first line has been fully loaded and its loading level cannot be further increased, it is impossible for the path to work at further higher loading level. Therefore, even the cascading gradient for a path may be large; the uneven distribution of power flow in the path may reduce its actual risk of cascading failure.

6. CASE STUDY

The assessment framework above is applied to the IEEE30-bus system and the IEEE118-bus system respectively. The parameters of the test systems are from the standard data set [34]. However, one important issue about capacities of transmission lines needs to be clarified. In [35][36][37], cascading failures were also simulated for IEEE standard testing systems. However, the capacities for transmission lines in these papers were still assumed proportional to the initial loads following equation (2). As discussed above, this assumption is not consistent with real situation of electrical engineering. In continuous operations of electrical power system, it is unreasonable to define the initial load. Under this assumption, different initial load distribution leads to different distribution of capacity and this is obviously not reasonable as the distribution of capacity is an intrinsic structural characteristic. In fact, the capacity of one transmission line mainly depends on the material of conductor, diameter and also environment conditions. If the environment conditions are neglected, for the lines of the same voltage level with same material of conductor and line size, which is the case for a typical IEEE test system, the capacities of these lines can be equal. Therefore, the capacities of lines in the test systems here are set equal.

The top 20 cascading paths with largest cascading gradients of IEEE30-bus system are identified as shown in Table II.
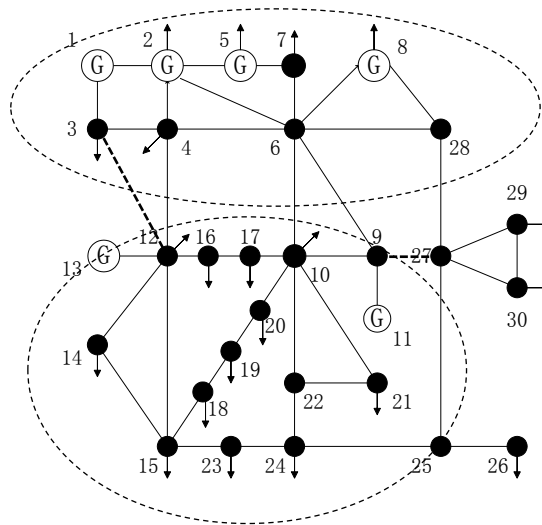

Fig. 5 The tested IEEE30-bussystem

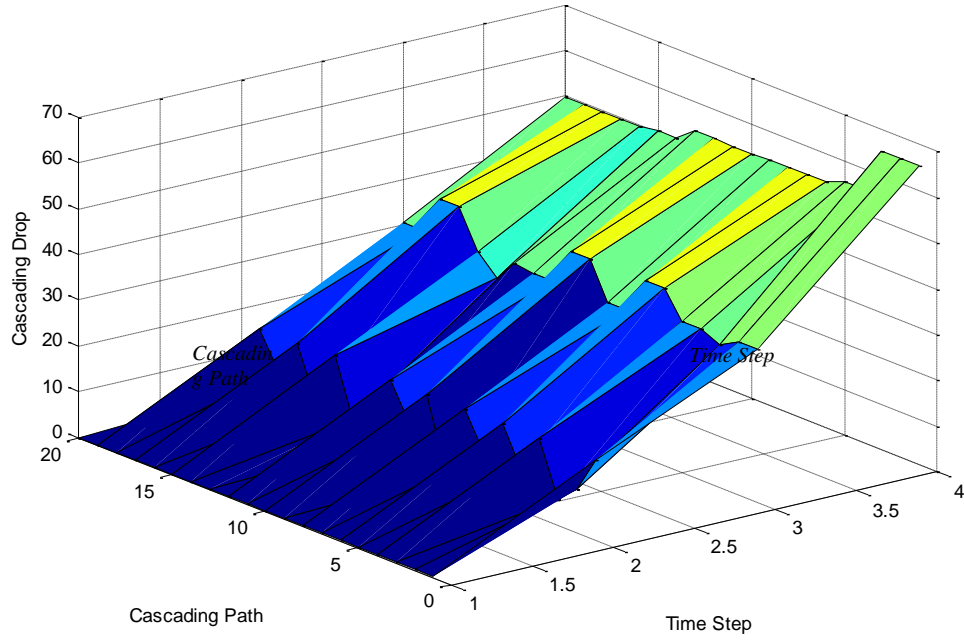The identified cascading paths are drawn in 3D and shown in figure 6.

Fig. 6 Top 20 cascading paths of the IEEE30-bus system

TABLE II

TOP 20 CASCADING PATHS FOR IEEE30-BUS SYSTEM

NO.	Cascading paths	Cascading gradient
1	*l(4,12)->l(9,10)->l(28,27)->l(6,10)*	21.7810
2	*l(9,10)->l(4,12)->l(28,27)->l(6,10)*	21.7810
3	*l(28,27)-> l(4,12)-> l(9,10)->l(6,10)*	21.7810
4	*l(4,12)->l(9,10)->l(25,27)->l(6,10)*	18.4477
5	*l(9,10)->l(4,12)->l(25,27)->l(6,10)*	18.4477
6	*l(4,12)->l(9,10) ->l(6,10)->l(28,27)*	17.9151
7	*l(9,10)->l(4,12)-> l(6,10)->l(28,27)*	17.9151
8	*l(4,12)-> l(6,10)-> l(9,10) ->l(28,27)*	17.9151
9	*l(6,10)-> l(4,12)->l(9,10)->l(28,27)*	17.9151
10	*l(4,12)->l(9,10)-> l(6,10)->l(25,27)*	17.8495
11	*l(9,10)->l(4,12)->l(6,10)->l(25,27)*	17.8495
12	*l(4,12)->l(6,10)->l(9,10)->l(25,27)*	17.8495
13	*l(6,10)->l(4,12)->l(9,10)->l(25,27)*	17.8495
14	*l(28,27)-> l(4,12)->l(6,9)->l(6,10)*	16.7810
15	*l(4,12)-> l(6,9)->l(28,27)->l(6,10)*	16.7810
16	*l(28,27)-> l(4,12)->l(6,10)->l(6,9)*	16.6591
17	*l(4,12)->l(9,10)->l(6,10)->l(24,25)*	16.6334
18	*l(9,10)->l(4,12)->l(6,10)->l(24,25)*	16.6334
19	*l(4,12)->l(6,10)-> l(9,10)->l(24,25)*	16.6334
20	*l(6,10)-> l(4,12)-> l(9,10)->l(24,25)*	16.6334

l(i,j) indicates the line connecting between bus *i* and bus *j*.

TABLE III
RESULTS OF CASCADING FAILURE TEST UNDER STATE1

NO.	R_{S1}^{H}	Cascading failure results
1	12.05757	$l^0(4,12)$-> $l^1(9,10)$-> $l^2(28,27)$,$l^2(6,10)$
2	12.05757	$l^0(9,10)$-> $l^1(4,12)$-> $l^2(28,27)$,$l^2(6,10)$
3	12.05757	$l^0(28,27)$-> $l^1(4,12)$-> $l^2(9,10)$->$l^3(6,10)$
4	9.72871	No cascading failure along this path.
5	9.72871	No cascading failure along this path.
6	9.91745	$l^0(4,12)$-> $l^1(9,10)$-> $l^2(28,27)$,$l^2(6,10)$
7	9.91745	$l^0(9,10)$-> $l^1(4,12)$-> $l^2(28,27)$,$l^2(6,10)$
8	9.91745	$l^0(4,12)$-> $l^1(9,10)$-> $l^2(28,27)$,$l^2(6,10)$
9	9.91745	$l^0(6,10)$-> $l^1(4,12)$->$l^2(9,10)$->$l^3(28,27)$
10	9.41325	No cascading failure along this path.
11	9.41325	No cascading failure along this path.
12	9.41325	No cascading failure along this path.
13	9.41325	No cascading failure along this path.
14	6.87452	No cascading failure along this path.
15	6.87452	No cascading failure along this path.
16	6.82455	No cascading failure along this path.
17	8.76766	No cascading failure along this path.
18	8.76766	No cascading failure along this path.
19	8.76766	No cascading failure along this path.
20	8.76766	No cascading failure along this path.

To evaluate the impact of operating states on the cascading paths and failure, two operating states are selected and under heavy and light loading levels as shown in figure 7 where power is given in per unit values.
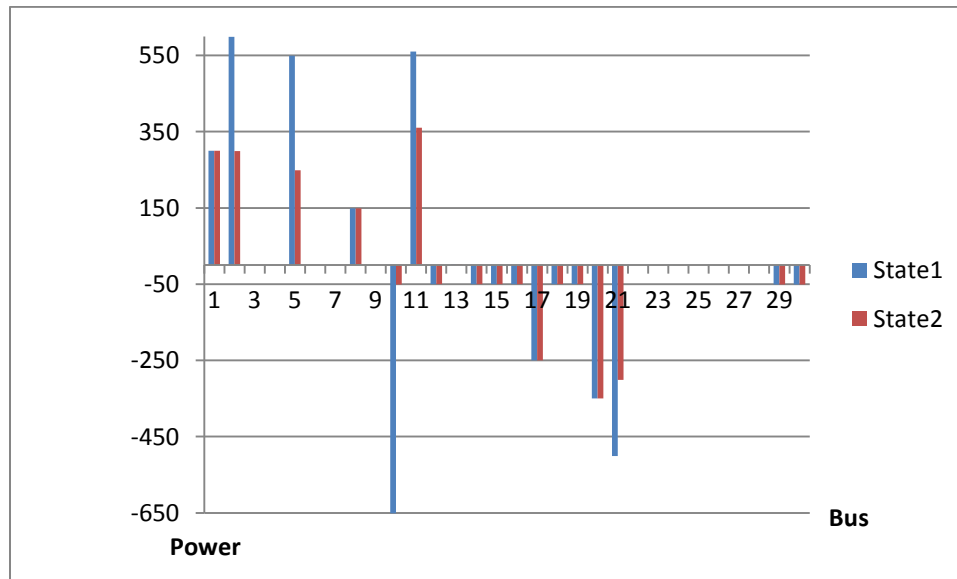

Fig. 7 Two tested operational states

In figure 7, positive power represents for generation and negative power for consumption.

To verify the cascading failure results, the DC power flow of each line under two different states in figure 6 are calculated. Then the first line in each path of Table II is initially removed respectively, and the DC power flow is recalculated subsequently. After the recalculation of power flow, if the power flow of any line exceeded its line flow limit, this line is removed and the recalculation is repeated. This procedure is continued until no overloaded line is found or the network was split into two disconnected sub-networks. In Table III, the results under state 1 of figure 7 are recorded, and the cascading risk of each path under state 1 is calculated.

In Table III, $l^t(i,j)$ indicates the line between bus i and bus j is removed at step t. For example, for path 1, the first line $l(4,12)$ is initially removed at step 0, and then the second line $l(9,10)$ in the path is removed due to overloading at step 1, then $l(28,27)$and $l(6,10)$ are removed simultaneously due to overloading at step 2. According to the results, for cascading paths with higher cascading risk, cascading failures are triggered along the paths. It is necessary to point out, if the loading level of lines in paths is

high enough, the remaining lines may be broken due to overloading simultaneously, but not in sequence of time steps as indicated in the paths. As cascading paths with gradients only indicate a general tendency, this phenomenon can still be regarded acceptable. Paths 4 and 5 with higher cascading gradient but lower cascading risk compared with paths 6-9 do not have a cascading failure along them. But cascading failures are detected along paths 6-9. These are consistent with the analysis according to the framework. For the other cascading paths with lower cascading risks, no cascading failures along the paths are detected. Furthermore, for state 2 of figure 7, the loading level and corresponding cascading risks for all paths have been significantly reduced, no cascading failures are detected under this state for all paths. These results are consistent with the idea in designing the cascading path and cascading risk. Even with high cascading gradient, cascading risk is low due to light loading level and no cascading failure has been detected.

According to the definition of cascading gradient of network in (10), the cascading gradient for the IEEE30-bus system is:
$$G^Y = 21.781$$

In fact, as shown in figure 4, the IEEE30-bus system can be divided as two regions which are indicated by two circles in broken lines. Most generation buses locate in region 1 and most load buses locate in region 2. Therefore, the power transmission would heavily depend on the lines connecting these two regions. Most lines of the identified top 20 cascading paths locate at the borders of these two regions. That means, due to the structural reason, cascading failures propagating in these lines have higher probabilities. Of course, such cascading failures due to the fact that heavy loading levels exist in these lines in operation.

Furthermore, to mitigate this structural vulnerability, according to the analysis above, two lines $l(3,12)$ and $l(9,27)$ are added to the border of these two regions in the network. The new network is indicated as $Y+$. The cascading gradient for the new network is:
$$G^{Y+} = 13.784$$

Therefore, by analysis of structural vulnerability and corresponding improvement, the identified cascading failure vulnerability can be significantly mitigated.

However, if we assume the line $l(9,10)$ is out of operation due to maintenance, the corresponding network is indicated as $Y-$. The cascading gradient for the network is:
$$G^{Y-} = 30.948$$

The removal of some critical component will have a great impact on the network due to the arising potential vulnerability related to cascading failure. This approach can help to make an overall evaluation for cascading failure for any change in structure.

Furthermore, the top 20 cascading paths with largest cascading gradients of the IEEE118-bus system were identified as shown in Table IV.

TABLE IV
TOP 20 CASCADING PATHS FOR IEEE118-BUS SYSTEM

NO.	Cascading Paths	Cascading gradient
1	$l(65,68)->l(47,69)->l(23,24)->l(49,69)$	410.3058
2	$l(65,68)->l(49,69)->l(23,24)->l(47,69)$	401.7609
3	$l(68,81)->l(69,77)->l(75,118)->l(75,77)$	320.4143
4	$l(81,80)->l(69,77)->l(75,118)->l(75,77)$	320.4143
5	$l(65,68)->l(49,69)->l(23,24)->l(47,49)->l(46,47)$	319.7799
6	$l(65,68)->l(49,69)->l(47,49)->l(23,24)->l(46,47)$	319.7799
7	$l(68,81)->l(69,77)->l(75,77)->l(75,118)$	310.0649
8	$l(81,80)->l(69,77)->l(75,77)->l(75,118)$	310.0649
9	$l(68,81)->l(69,77)->l(76,118)->l(75,77)$	308.4143
10	$l(81,80)->l(69,77)->l(76,118)->l(75,77)$	308.4143
11	$l(68,81)->l(69,77)->l(76,77)->l(75,77)$	307.081
12	$l(81,80)->l(69,77)->l(76,77)->l(75,77)$	307.081
13	$l(81,80)->l(69,77)->l(75,77)->l(76,77)$	304.0507
14	$l(68,81)->l(69,77)->l(75,77)->l(76,77)$	304.0507
15	$l(65,68)->l(49,69)->l(23,24)->l(47,49)->l(47,69)$	301.3207
16	$l(65,68)->l(49,69)->l(47,49)->l(23,24)->l(47,69)$	301.3207
17	$l(81,80)->l(68,69)->l(47,69)->l(23,24)->l(49,69)$	299.2293
18	$l(68,81)->l(68,69)->l(47,69)->l(23,24)->l(49,69)$	299.2293
19	$l(81,80)->l(69,77)->l(75,77)->l(76,118)$	298.954
20	$l(68,81)->l(69,77)->l(75,77)->l(76,118)$	298.954

$l(i,j)$ indicates the line connecting between bus i and bus j.

The maximum gradient of path 1 can be converted with reference to the IEEE30-bus system by equation (11):

$$410.3058 \times (GL_{IEEE30}/GL_{IEEE118}) = 9.671$$

The structure of the IEEE118-bus system is much better than the IEEE30-bus system in terms of the cascading failure tendency.

An operating state of IEEE118-bus system has been used for test, where the maximum loading level of the path with the maximum gradient is about 55%, which is similar to the loading level of the path with maximum gradient in state 1 for the IEEE30-bus system in table III. The first line of each path in table IV is cut off, no cascading failure is detected through the corresponding path. This is consistent with the former result that the structure of IEEE118-bus system is better than that of the IEEE30-bus system for cascading tendency. Due to uneven distribution of power flow, it is difficult for this system to operate on a much higher loading level in normal operation. Therefore, the total cascading risk of this system is relatively low.

In comparison, IEEE118-bus system is also applied to evaluate the cascading failure in [35][36][37] based on their specific models respectively. However, the simulations in these studies cannot give concrete conclusions. In addition, the pure structural cascading tendency and the impact of loading level discussed here could not be evaluated in these models. As discussed before, they still followed the assumption of capacities in equation (2), and even made analysis for cascading characteristics corresponding to different tolerance factors. But as this tolerance factor does not exist in real power systems, the results could not provide effective supports to power system operation.

With the simulation results from these two test systems, the proposed framework has been preliminarily justified for its effectiveness and validity. Under this framework, the dedicated metrics defined as cascading gradient and loading level have been verified as an effective tool to evaluate the cascading tendency and the triggering force in the model. Furthermore, the simulation results can also support the three statements made in section 3.

7. Conclusion

People have worked for a long time to analyze cascading failures in power grids based on complex networks from the structural perspective to enhance the protection capability of the grids from this destructive disaster. However, former studies still cannot provide meaningful guidance for practical power system operation due to lack of clear understanding on the relations of structure and operational states, as well as unreasonable assumptions with reference to electrical engineering in those analysis models.

There are two main contributions of this paper. The first one is to propose a framework for the study of cascading failure to distinguish and evaluate the relationships between structure and operational states; the second one is to define two evaluation metrics to indicate the cascading tendency and triggering force in the framework. Furthermore, the cascading risk can be quantitatively assessed by integrating these two metrics.

In case study, preliminary results were obtained to demonstrate the effectiveness of the proposed metrics. Simulation results implies that the proposed model can identify the most dangerous cascading paths according to structure in advance, and the risk of cascading failures based on such vulnerabilities can be assessed by monitoring the loading level of these cascading paths. Measures to mitigate structural vulnerabilities can be obtained and impacts of structural adjustments related to cascading failures can be assessed by this model.

However, there is still a long way to improve this model for real system operation. The real procedure of cascading failures in power grids is very complex and involves a large number of components and systems. The model in terms of cascading gradient and loading level is only one way to realize the proposed framework. Another object of this paper is to encourage more solutions within the framework of interrelation between structure and operational states. We believe that in our future work, better metrics indicating cascading tendency and triggering force could be found in the future, and better algorithms to detect most critical cascading paths more efficiently need to be developed. Following that, the analysis based on the interrelation of structure and operational states will provide more effective guidance for system operation.

Acknowledgement

References

[1] E. Bompard, C. Gao, M. Masera, R. Napoli, A. Russo, A. Stefanini, and F. Xue, *Approaches To The Security Analysis Of Power Systems: Defence Strategies Against Malicious Threats*, Luxembourg: Office for Official Publications of the European Communities, 2007, EUR 22683 EN, ISSN 1018-5593

[2] M. Vaiman, K. Bell, Y. Chen, B. Chowdhury, I. Dobson, P. Hines, M. Papic, S. Miller, P. Zhang, Risk Assessment of Cascading Outages: Methodologies and Challenges, *IEEE Transactions on Power Systems*, 2012, Volume: 27, Issue: 2 Pages: 631 - 641.

[3] M.J. Eppstein, P.D.H. Hines, A "Random Chemistry" Algorithm for Identifying Collections of Multiple Contingencies That Initiate Cascading Failure, *IEEE Transactions on Power Systems*, 2012, volume: 27, Issue: 3 Pages: 1698 – 1705.

[4] Shan Liu, Bo Chen, T. Zourntos, D. Kundur, K. Butler-Purry, A Coordinated Multi-Switch Attack for Cascading Failures in Smart Grid, *IEEE Transactions on Smart Grid*, 2014, Volume: 5, Issue: 3 Pages: 1183 – 1195.

[5] Shengwei Mei, YixinNi, Gang Wang, Shengyu Wu, A Study of Self-Organized Criticality of Power System Under Cascading Failures Based on AC-OPF With Voltage Stability Margin, *IEEE Transactions on Power Systems*, 2008, Volume: 23, Issue: 4 Pages: 1719 – 1726.

[6] P.Henneaux, P.-E. Labeau, J.-C. Maun, L.Haarla, A Two-Level Probabilistic Risk Assessment of Cascading Outages, *IEEE Transactions on Power Systems*, 2015, Volume: PP, Issue: 99 Pages: 1 – 11.

[7]   Junjian Qi, Kai Sun, Shengwei Mei, An Interaction Model for Simulation and Mitigation of Cascading Failures, *IEEE Transactions on Power Systems*, 2015, Volume: 30, Issue: 2 Pages: 804 – 819.

[8]   Janghoon Kim, I.Dobson,Approximating a Loading-Dependent Cascading Failure Model With a Branching Process, IEEE Transactions on Reliability, 2010, Volume: 59, Issue: 4 Pages: 691 – 699.

[9]   Jun Yan, Yufei Tang, Haibo He, Yan Sun, Cascading Failure Analysis With DC Power Flow Model and Transient Stability Analysis, *IEEE Transactions on Power Systems*, 2015, Volume: 30, Issue: 1 Pages: 285 – 297.

[10]   Quan Chen, L.Mili, Composite Power System Vulnerability Evaluation to Cascading Failures Using Importance Sampling and AntitheticVariates,*IEEE Transactions on Power Systems*, 2013, Volume: 28, Issue: 3 Pages: 2321 – 2330.

[11]   P.Rezaei, P.D.H. Hines, M.J. Eppstein, Estimating Cascading Failure Risk With Random Chemistry,*IEEE Transactions on Power Systems*, 2015, Volume: 30, Issue: 5 Pages: 2726 – 2735.

[12]   Pierre Henneaux, Probability of failure of overloaded lines in cascading failures, *Electrical Power and Energy Systems*, 73 (2015),Pages: 141–148

[13]   M. Rahnamay-Naeini, ZhuoyaoWang,N. Ghani, A. Mammoli, M.M.Hayat, Stochastic Analysis of Cascading-Failure Dynamics in Power Grids,*IEEE Transactions on Power Systems*, 2014, Volume: 29, Issue: 4 Pages: 1767 – 1779.

[14]   D. J. Watts, S. H. Strogatz, Collective dynamics of small-world networks, *Nature*, 1998, 393(6684), Pages:440–442.

[15]   A.-L. Barab ási, R. Albert, Emergence of scaling in random networks, *Science*, 1997, 286, Pages: 509–512.

[16]   Marti Rosas-Casals, SergiValverde,Ricard V. Sole, Topological Vulnerability of the European Power Grid Under Errors and Attacks, *International Journal of Bifurcation and Chaos*, Vol. 17, No. 7 (2007) Pages: 2465-2475.

[17]   Reka Albert, Istvan Albert and Gray L. Nakarado, Structural vulnerability of the North American power grid, *Physical Review E* 69, 025103(R) (2004).

[18]   David P. Chassin and Christian Posse, Evaluating North American electric grid reliability using the Barabasi-Albert network model, *PhysicaA* 355 (2005), Pages: 667-677.

[19]   Vito Latora& Massimo Marchiori, Vulnerability and protection of infrastructure networks, *Physical Review E* 71, 015103(R) (2005).

[20]   Paolo Crucitti, Vito Latora and Massimo Marchiori, Locating Critical Lines in High-Voltage Electrical Power Grids, *Fluctuation and Noise Letters*, Vol.5, No. 2 (2005) L201-L208.

[21]   Gao J, Buldyrev S V, Stanley H E, et al. Networks formed from interdependent networks [J]. Nature physics, 2012, 8(1): 40-48.

[22]   Paolo Crucitti, Vito Latora& Massimo Marchiori, Model for cascading failures in complex networks, *PHYSICAL REVIEW E* 69, 045104(R) (2004)

[23]   Adilson E. Motter& Ying-Cheng Lai, Cascade-based attacks on complex networks, *PHYSICAL REVIEW E* 66, 065102(R) (2002)

[24]   Paolo Crucittia, Vito Latorab, Massimo Marchioric& Andrea Rapisardab, Error and attack tolerance of complex networks, *Physica A* 340 (2004),Pages:388 – 394.

[25]   Ryan Kinney, Paolo Crucitti, Reka Albert and Vito Latora, Modeling Cascading Failures in the North American Power Grid, *Eur. Phys. J. B* 46 (2005)101.

[26]   Paolo Crucitti, Vito Latora, Massimo Marchiori, A topological analysis of the Italian electric power grid, *Physica A* 338 (2004) Pages:92-97.

[27]   S. Arianos, E. Bompard, A. Carbone, F. Xue, Power grid vulnerability: A complex network approach, *Chaos* 19, 013119 (2009).

[28]   Ettore Bompard, Roberto Napoli,Fei Xue, Analysis of structural vulnerabilities in power transmission grids, International Journal of Critical Infrastructure Protection, Volume 2, Issues 1–2, May 2009, Pages:5–12.

[29]   E.Bompard, R. Napoli, F. Xue, Extended topological approach for the assessment of structural vulnerability in transmission networks, IET Generation, Transmission & Distribution, Volume:4, Issue: 6, Pages:716 – 724.

[30]   Ettore Bompard, Di Wu, Fei Xue, Structural vulnerability of power systems: A topological approach, *Electric Power Systems Research*, Volume 81, Issue 7, July 2011, Pages: 1334–1340.

[31]   Jun Yan, Haibo He, Yan Sun, Integrated Security Analysis on Cascading Failure in Complex Networks, *IEEE Transactions on Information Forensics and Security*, 2014, Volume: 9, Issue: 3 Pages: 451 – 463.

[32]   Yihai Zhu, Jun Yan, Yan Sun, Haibo He, Revealing Cascading Failure Vulnerability in Power Grids Using Risk-Graph,*IEEE Transactions on Parallel and Distributed Systems*, 2014, Volume: 25, Issue: 12 Pages: 3274 – 3284.

[33]   YakupKo ç, MartijnWarnier, Robert E. Kooij, Frances M.T. Brazier, An entropy-based metric to quantify the robustness of power gridsagainst cascading failures, *Safety Science*, 59 (2013) Pages:126–134.

[34]   IEEE Test Systems Data. <http://www.ee.washington.edu/research/pstca/>.

[35]   YuanYu Dai, GuoChenc,d, ZhaoYang Dong, YuSheng Xue, David J. Hill, Yuan Zhao, An improved framework for power grid vulnerability analysis considering critical system features, Physica A 395 (2014) 405–415.

[36]   YakupKo ç, MartijnWarnier, Robert E. Kooij, Frances M.T. Brazier, An entropy-based metric to quantify the robustness of power grids against cascading failures, Safety Science 59 (2013) 126–134.

[37]   Guo Chena, Zhao Yang Dong, David J. Hill, Guo Hua Zhang, Ke Qian Hua, Attack structural vulnerability of power grids: A hybrid approach based on complex networks, Physica A 389 (2010) 595-603.

F. Xue was born in 1977 in Tonghua of Jilin province in China. He received his Bachelor and Master degrees in power system and its automation from Wuhan University in China in 1999 and 2002, respectively. He received the Ph.D. of Electrical Engineering degree from the Department of Electrical Engineering of Politecnico di Torino, Torino, Italy, 2009.

He was the Deputy Chief Engineer of Beijing XJ Electric Co.,Ltd and Lead Research Scientist in Siemens Eco-City Innovation Technologies (Tianjin) Co., Ltd. He is currently with the Department of Electrical and Electronic Engineering, Xi'an Jiaotong-Liverpool University, No. 111 Ren'ai Road, Suzhou Industrial Park, Suzhou, P.R. China.

His research interest focuses on power system security, integration of wind power into power grids, electric vehicle and energy internet.